Pergamon

Bioorganic & Medicinal Chemistry 10 (2002) 713–718

BIOORGANIC & MEDICINAL CHEMISTRY

Modulation of Remote DNA Oxidation by Hybridization with Peptide Nucleic Acids (PNA)

Akimitsu Okamoto, Kazuhito Tanabe, Chikara Dohno and Isao Saito*

Department of Synthetic Chemistry and Biological Chemistry, Faculty of Engineering, Kyoto University, and CREST, Japan Science and Technology Corporation, Kyoto 606-8501, Japan

Received 3 August 2001; accepted 8 September 2001

Abstract—We have examined the efficiency of DNA photooxidation in DNA/PNA duplex and DNA/$(PNA)_2$ triplex for the first time. DNA/PNA duplex was cleaved at GG steps by external riboflavin with high efficiency like specific GG cleavage in DNA/DNA duplex. However, the 5′G selectivity of the GG oxidation in DNA/PNA duplex was much lower than that observed in DNA/DNA duplex. Remote DNA oxidation of oxidant-tethered DNA/PNA duplex was considerably suppressed. In contrast, the formation of DNA/$(PNA)_2$ triplex by hybridization with two PNA strands completely inhibited the remote GG oxidation, indicating that PNA acts as an inhibition for remote oxidative DNA damage.

Introduction

Stacked bases in DNA duplex provide an effective media for long-range charge transport through DNA.[1–6] Oxidative DNA damage caused by metabolism,[7] UV irradiation,[8] gamma-ray,[9] and pulse radiolysis[10] is accumulated at guanine base (G) which has the lowest oxidative potential among nucleobases.[11] Particularly, GG doublet is more easily oxidized than single G, since oxidation potentials of GN sequences are in the order of GG > GA > > GC and GT.[12,13] Recently, it has been suggested that the long-range hole migration proceeds via a multistep hole-hopping mechanism and the efficiency of long-range hole migration is strongly affected by the sequence intervening between hole donor and acceptor.[5,6,14–17] The long-range hole migration through DNA triplex has also been reported.[18,19]

Peptide nucleic acid (PNA) is a nucleic acid analogue possessing peptide backbone instead of sugar-phosphate backbone.[20] PNA oligomer is known to tightly bind to complementary DNA and RNA, forming right-handed duplex.[21] While DNA/PNA duplex has been intensively studied with regard to the hybridized structures and thermodynamics, little is known on the chemical reactivity of DNA/PNA duplex and DNA/$(PNA)_2$ triplex. Schuster et al. reported long-range hole migration through DNA/PNA duplex containing anthraquinone unit.[22,23]

As a general problem for the hybridization of DNA with PNA, elucidation of how the chemical reactivity of DNA is altered as a result of hybridization with PNA is very important. Particularly, we are very interested in the potential use of PNA as an inhibitor for remote oxidative DNA lesion. Herein, we report how the efficiency of GG oxidation is altered by hybridization with PNA. In this study, two types of guanine oxidation were examined; one is the photooxidation with an external one-electron photosensitizer such as riboflavin and the other is the remote oxidation with oxidant-tethered DNA. It was found that DNA/PNA duplex was cleaved at GG step of DNA strand by external riboflavin with high efficiency like GG cleavage in DNA/DNA duplex. However, the 5′G selectivity of the GG oxidation in DNA/PNA duplex was lower than that observed in DNA duplex. On the other hand, in the photooxidation of DNA/PNA duplex using an oxidant-tethered DNA strand, the efficiency of the remote GG oxidation in DNA/PNA duplex was considerably suppressed. Remote oxidation through DNA/$(PNA)_2$ triplex containing GG step in the DNA strand was also investigated. It was demonstrated for the first time that the triplex formation with two PNA strands result in an almost complete inhibition of the remote GG oxidation. The present results suggest a possibility for the use of PNA as an inhibitor for long-range oxidative DNA lesion.

*Corresponding author. Tel.: +81-75-753-5656; fax: +81-75-753-5676; e-mail: saito@sbchem.kyoto-u.ac.jp

0968-0896/02/$ - see front matter
PII: S0968-0896(01)00320-0

Results and Discussion

DNA and PNA strands used in this study are shown in Table 1. 13 mer **DNA 2a** and **2b** were complementary to 5′ side part of 21 mer **DNA 1**, and 8 mer **DNA 3** and **PNA 3a** and **3b** were complementary to 3′ side part of **DNA 1**. **X** in **DNA 2b** denotes cyanobenzophenone-substituted 2′-deoxyuridine.[24] **DNA 4a** contains a polypurine region, which forms a triplex with 8 mer polypyrimidine strands **DNA 5a**, **5b** and **PNA 5**. PNA strands were synthesized according to a conventional ᵗBoc solid phase peptide synthesis,[25] and their compositions were confirmed by MALDI-TOF mass spectrometry. The melting temperatures (T_m) of duplexes and triplexes measured by absorption at 260 nm were shown in Table 2. The circular dichromism (CD) spectra of the duplexes and triplexes were all consistent with those reported previously.[26]

We first examined the photooxidation of DNA strand in DNA/PNA duplex by an external oxidant and compared the oxidation efficiency and selectivity with those for DNA/DNA duplex. The duplexes containing ^{32}P-5′-end-labeled DNA were irradiated at 366 nm in the presence of riboflavin as a photosensitizer at 0 °C for 1 h. The reaction was analyzed by polyacrylamide gel electrophoresis after hot piperidine treatment. The result was shown in Figure 1a. The strong cleavage bands were observed at GG steps in DNA/DNA duplex (lane 3), antiparallel DNA/PNA duplex (lane 6) and parallel DNA/PNA duplex (lane 10) as a result of photoirradiation with riboflavin and hot piperidine treatment. The intensities of cleavage bands at $\mathbf{G_{16}G_{17}}$ steps in DNA/PNA duplexes were nearly equal to the band intensity at $\mathbf{G_{16}G_{17}}$ step in DNA/DNA duplex. However, the 5′G ($\mathbf{G_{16}}$) selectivity for the DNA cleavage of both antiparallel and parallel DNA/PNA duplexes was lower than that observed in DNA/DNA duplex. The results of Figure 1a indicated that the hybridization of PNA to DNA did not suppress the GG oxidation by riboflavin but a considerable loss of the 5′G selectivity was observed.

DNA oxidation initiated by a photosensitizer covalently linked to DNA was next investigated. Through these experiments we obtained an interesting result on the efficiency and selectivity of the long-range oxidative DNA lesion. **DNA 2b**, which contains cyanobenzophenone-substituted 2′-deoxyuridine (**X**) as an electron-accepting photosensitizer, was annealed with ^{32}P-labeled **DNA 1** containing GG site. The duplexes were irradiated at 312 nm at 0 °C for 1 h. The result of autoradiography was shown in Figure 1b. The ratio of cleavage band intensities at GG step in DNA/DNA duplex was very similar to that observed for riboflavin-sensitized photooxidation (lane 3 in Fig. 1b versus Fig. 1a). In contrast, the cleavage bands at $\mathbf{G_{16}G_{17}}$ step in antiparallel (lane 6) and parallel DNA/PNA duplex (lane 10) were smaller as compared with the $\mathbf{G_{16}G_{17}}$ bands in lane 3. These results suggest that the hybridization of PNA to DNA decreased the efficiency of the remote oxidation at $\mathbf{G_{16}G_{17}}$ step. Furthermore, the 5′G ($\mathbf{G_{16}}$) selectivity of the DNA cleavage at $\mathbf{G_{16}G_{17}}$ in DNA/PNA duplex was completely lost.

In order to gain an insight into the efficiency and site-selectivity for the GG oxidation, molecular orbital calculation of GG step in DNA/PNA duplex was examined. We built 5′-GG-3′/H-CC-NH_2 duplex using parameters for antiparallel DNA/PNA duplex previously reported,[27] and obtained HOMO energy and HOMO distribution of this duplex by means of B3LYP/6-31G(d) calculation. The HOMO energy of 5′-GG-3′/H-CC-NH_2 duplex was −4.50 eV. This is slightly smaller than that of DNA/DNA duplex 5′-GG-3′/3′-CC-5′ (−4.44 eV). The calculated HOMO energy suggests that like GG step of DNA/DNA duplex the GG step of DNA/PNA duplex is also oxidizable by one-electron oxidant with a similar high efficiency. The 5′G/3′G ratio of calculated HOMO distribution on GG step in DNA/PNA duplex was 100:57, which was smaller than that for DNA/DNA duplex (100:40) (Fig. 2). These calculation data were consistent with the cleavage pattern actually obtained in the DNA oxidation with riboflavin, although the calculation data of small DNA/PNA model in a gas phase does not always correctly reflect the real photooxidation rate and selectivity in aqueous media.

The strong cleavage bands were observed at GG step in DNA/DNA duplex regardless of oxidation methods, whereas the GG cleavage in DNA/PNA duplex was considerably suppressed when the photooxidation was carried out with an internal cyanobenzophenone photosensitization in spite of the effective GG cleavage by riboflavin. This implies that the remote DNA oxidation

Table 1. DNA and PNA strands used in this study

	Sequences[a]
DNA	5′-(^{32}P)-ATTTATAG$_8$TA**G$_{11}$G$_{12}$**TCT**G$_{16}$G$_{17}$**ACAC-3′
DNA 2a	3′-TAAATATCATCCA-5′
DNA 2b	3′-TAAATA**X**CATCCA-5′
DNA 3	3′-GACCTGTG-5′
PNA 3a	H_2N-GACCTGTG-H
PNA 3b	H-GACCTGTG-NH_2
DNA 4a	5′-(^{32}P)-ATTTATAG$_8$TA**G$_{11}$G$_{12}$**TAG$_{15}$AA**G$_{18}$G$_{19}$**AA-3′
DNA 4b	5′-AGAAGGAA-3′
DNA 5a	5′-TCTTCCTT-3′
DNA 5b	3′-TCTTCCTT-5′
PNA 5	H_2N-TCTTCCTT-H

[a]**X** is cyanobenzophenone-substituted 2′-deoxyuridine; NH_2 is carboxyamide end of PNA; H is amino end of PNA.

Table 2. Melting temperatures (T_m) of duplexes and triplexes

	T_m (°C)
Duplex[a]	
DNA/DNA 2a	19
DNA/(DNA 2a + DNA 3)	23[b]
DNA/(DNA 2a + PNA 3a)	25, 44
DNA/(DNA 2a + PNA 3b)	19, 42
Triplex[c]	
DNA 4b/DNA 5a/DNA 5b	8, 31
DNA 4b/(PNA 5)$_2$	64[b]

[a]Conditions: 2.5 μM duplex, 10 mM sodium cacodylate, pH 7.0.
[b]Only one sigmoidal curve was observed.
[c]Conditions: 2.5 μM triplex, 10 mM sodium cacodylate, pH 6.2.

through DNA/PNA duplex is less efficient than in DNA/DNA duplex. First of all, structural studies of DNA/PNA duplex indicate that the conformation is quite different from B-form DNA/DNA duplex.[27] In particular, the base stacking of DNA/PNA duplex is significantly different from B-form DNA duplex. In addition, the local structural changes could also occur not only in DNA/PNA duplex region but also at the DNA–PNA junction site as already observed at the DNA–RNA junction.[28] Thus, the change of the elec-

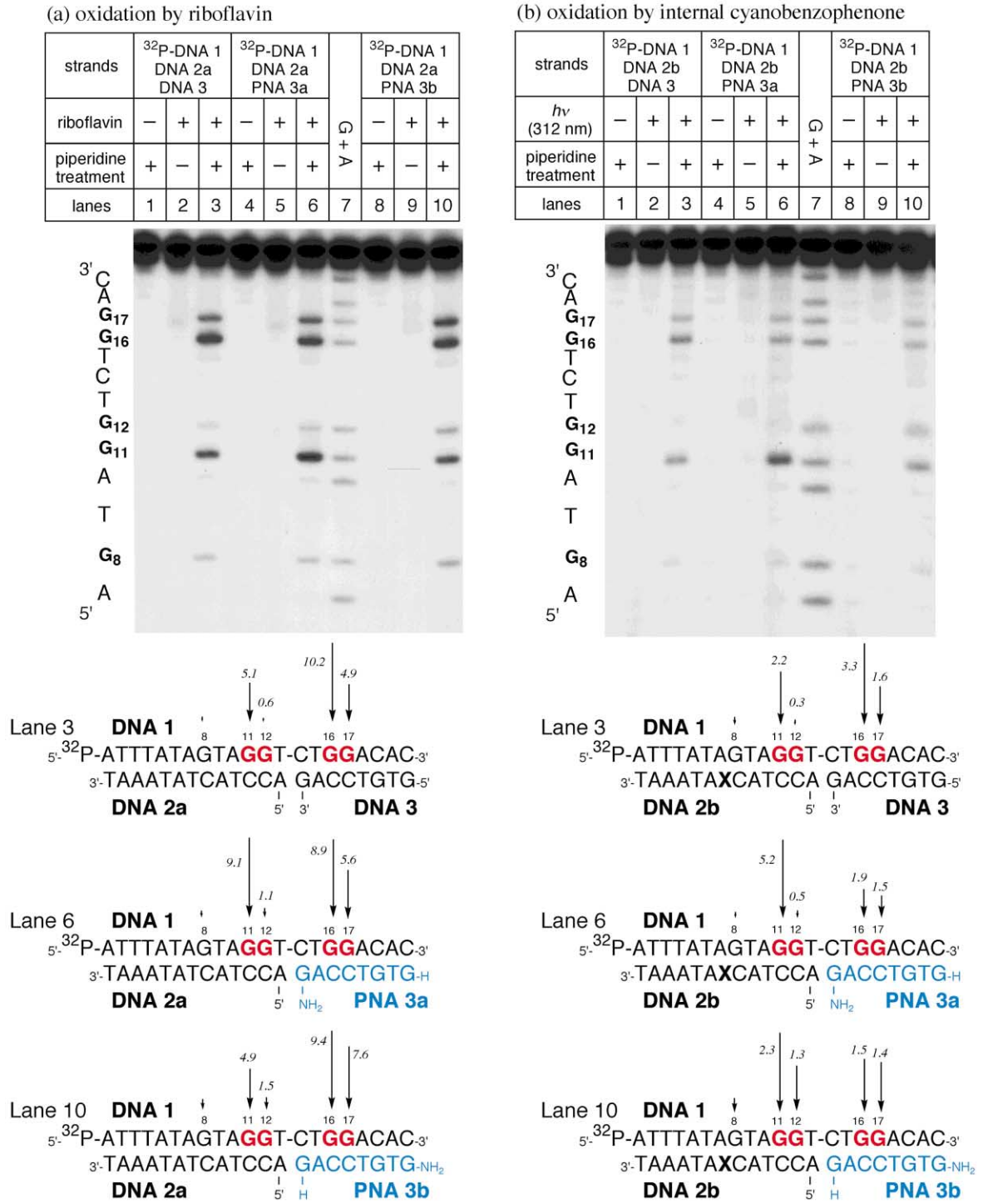

Figure 1. Autoradiograms of a denaturing gel electrophoresis for ^{32}P-5′-end labeled **DNA 1** after photooxidation of the duplexes. (a) 366 nm photoirradiaton of duplexes in the presence and absence of riboflavin at 0 °C for 1 h followed by hot piperidine treatment (90 °C, 20 min). Lanes 1–3, **DNA**/(**DNA 2a** + **DNA 3**); lanes 4–6, **DNA**/(**DNA 2a** + **PNA 3a**); lane 7, Maxam-Gilbert G + A sequencing lane; lanes 8–10, **DNA**/(**DNA 2a** + **PNA 3b**). (b) 312 nm photoirradiaton of duplexes containing cyanobenzophenone-substituted 2′-deoxyuridine (**X**) incorporated into **DNA 2b** at 0 °C for 1 h followed by hot piperidine treatment (90 °C, 20 min). Lanes 1–3, **DNA**/(**DNA 2b** + **DNA 3**); lanes 4–6, **DNA**/(**DNA 2b** + **PNA 3a**); lane 7, Maxam-Gilbert G + A sequencing lane; lanes 8–10, **DNA**/(**DNA 2b** + **PNA 3b**). The arrows and italic numbers represent relative intensities of cleavage bands obtained by densitometric analysis.

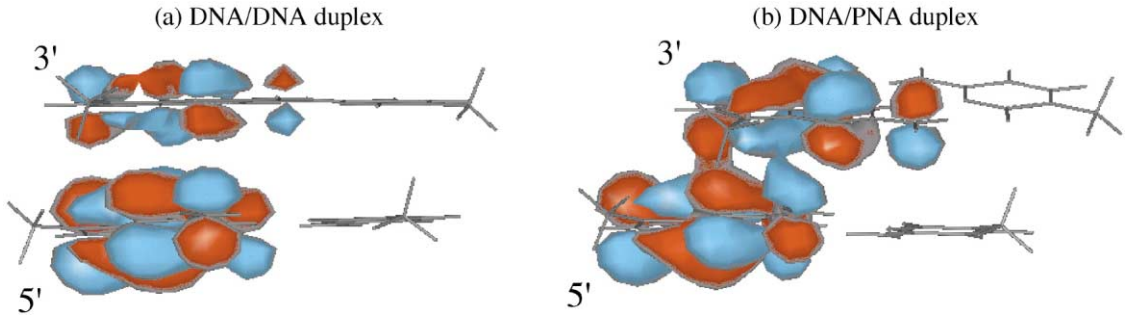

Figure 2. Orbital contour plots of the HOMOs of 5′-GG-3′/5′-CC-3′ and 5′-GG-3′/H-CC-NH_2 obtained by B3LYP/6-31G(d) calculation. The sugar phosphate backbones and polypeptide backbones were replaced by methyl group.

tronic overlap of the stacked bases in DNA/PNA hybrid as a result of structural alternations would cause the difference in the remote DNA oxidation efficiency.

In order to know the effect of triplex formation, we examined the photooxidation of DNA/$(PNA)_2$ triplex and compared the photooxidation efficiency with that of DNA triplex. The triplexes containing ^{32}P-5′-end-labeled DNA, shown in Figure 3, were irradiated at 312 nm. While the cleavage bands at $\mathbf{G_{18}G_{19}}$ in the DNA triplex region were ca. 20% of $\mathbf{G_{11}G_{12}}$ in DNA duplex region (lane 3), the cleavage bands at $\mathbf{G_{18}G_{19}}$ in the DNA/$(PNA)_2$ triplex region (lane 6) were dramatically reduced and almost negligible, indicating that the triplex formation of DNA with two PNA strands completely suppressed the DNA cleavage as compared with DNA triplex. The extremely weak DNA cleavage in remote GG oxidation of DNA/$(PNA)_2$ triplex would also be due to the structural change caused by the hybridization of PNA to DNA as well as to the decrease of solvent accessibility by triplex formation.

Conclusion

In summary, the DNA/PNA duplex was oxidized at GG step in the photooxidation with external riboflavin, whereas the efficiency of the remote GG oxidation was significantly lowered by the formation of DNA/PNA duplex. In addition, it was found that the hybridization of PNA to DNA resulted in a decrease of the 5′G selectivity of GG oxidation regardless of the oxidation methods used. Furthermore, the formation of the DNA/$(PNA)_2$ triplex almost completely suppressed DNA cleavage derived from the remote GG oxidation. Thus, PNA acts as an effective inhibitor for remote DNA oxidation by hybridization to DNA and is used as a useful tool for the study on the mechanism of oxidative DNA lesion.

Experimental

General techniques

Cyanobenzophenone-tethered oligodeoxynucleotides were synthesized as described elsewhere[24] on Applied Biosystems 392 DNA/RNA synthesizer. T4 kinase was purchased from NIPPON GENE (10 units/μL) and γ;-[^{32}P]-ATP (10 mCi/mL) was from Amersham Pharmacia Biotech. Photoirradiation at 312 or 366 nm was carried out using a Cosmo BIO CSF-20AF transilluminator. A Gibco BRL Model S2 sequencing gel electrophoresis apparatus was used for polyacrylamide gel electrophoresis (PAGE).

Synthesis and characterization of PNA oligomers

PNA oligomers were synthesized by solid-phase ^{t}Boc chemistry on a MBHA resin as described by Koch et al.[25] After the completion of PNA oligomer synthesis, the resin was treated with a solution of trifluoroacetic acid, trifluoromethanesulfonic acid, thioanisole, and *p*-cresol (6:2:1:1 v/v/v/v) for the cleavage of PNA oligomer from the resin and for the deprotection. The solution was filtered and precipitated in ethyl ether, centrifuged, and decanted. The residue was redissolved in trifluoroacetic acid, reprecipitated in ethyl ether, centrifuged, and then decanted to give the crude product. The crude oligomer was purified by reversed phase HPLC on a Wakosil II 5-C18-AR (20×150 mm) using a linear gradient of acetonitrile including 0.05% trifluoroacetic acid and aqueous 0.05% trifluoroacetic acid solvent system at a flow rate 4.0 mL/min and eluting products were detected by UV at 260 nm. Each **PNA** oligomer was characterized by MALDI-TOF MS; **PNA 3a** H-GTGTCCAG-NH_2, *m*/*z* 2202.82 (calcd for $[M+H]^+$ 2202.12); **PNA 3b** H-GACCTGTG-NH_2, *m*/*z* 2202.78 (calcd for $[M+H]^+$ 2202.12); **PNA 5** H-TTCCTTCT-NH_2, *m*/*z* 2103.26 (calcd for $[M+H]^+$ 2103.05).

T_m measurement

A 2.5 μM solutions of the appropriate oligonucleotides and PNA oligomers in 10 mM phosphate buffer (pH 7.0 for duplex, pH 6.2 for triplex) were prepared. Melting curves were obtained by monitoring the absorbance at 260 nm as the temperature was ramped from 2 to 81 °C at a rate of 1 °C/min.

Preparation of 5′-^{32}P-end-labeled ODN

Oligonucleotides (ODNs, 400 pmol strand concentration) were labeled by phosphorylation with 4 μL of [γ-^{32}P]ATP and 4 μL of T_4 polynucleotide kinase using standard procedures.[29,30] The 5′-end-labeled oligonucleotides were recovered by ethanol precipitation and

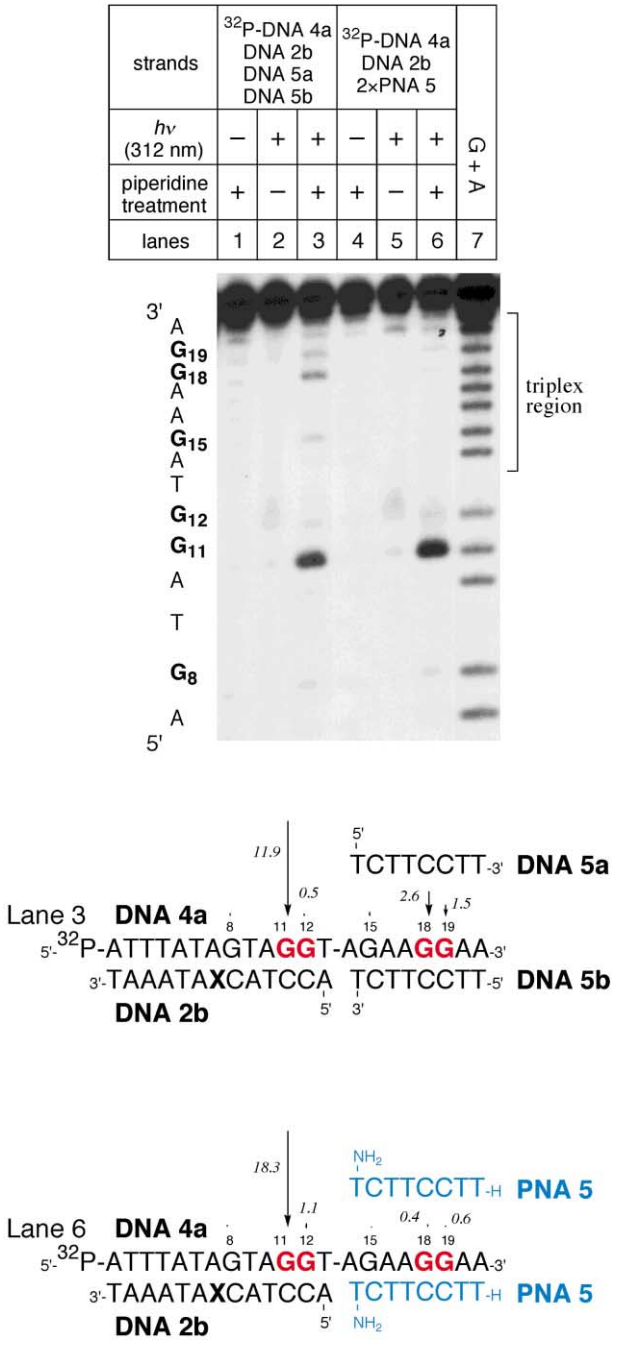

Figure 3. Autoradiograms of a denaturing gel electrophoresis for ^{32}P-5′-end labeled **DNA 4a** after photooxidation of triplexes. 312 nm photoirradiaton of triplexes containing cyanobenzophenone-substituted 2′-deoxyuridine (**X**) incorporated into **DNA 2b** at 0 °C for 1 h followed by hot piperidine treatment (90 °C, 20 min). Lanes 1–3, **DNA 4a**/(**DNA 2b** + **DNA 5a** + **DNA 5b**); lanes 4–6, **DNA 4a**/(**DNA 2b** + 2×**PNA 5**); lane 7, Maxam-Gilbert G + A sequencing lane. The arrows and italic numbers represent relative intensities of cleavage bands obtained by densitometric analysis.

further purified by 15% nondenaturing gel electrophoresis and isolated by the crush and soak method.[13]

Cleavage of ^{32}P-5′-end-labeled ODNs by photoirradiation in the presence of riboflavin

Sample solutions were prepared by hybridizing a mixture of cold and radiolabeled oligonucleotides (**DNA**, 1 μM) with 1 μM of **DNA 2a** and 1 μM of **DNA 3**, **PNA 3a** or **PNA 3b** in sodium phosphate buffer (pH 7.0). Hybridization was achieved by heating the sample at 90 °C for 5 min and slowly cooling to room temperature. The ^{32}P-5′-end-labeled ODN duplex (2.0×10^5 cpm) containing riboflavin was irradiated at 366 nm at 0 °C for 60 min. After irradiation, all reaction mixtures were precipitated with addition of 10 μL of *herring sperm* DNA (1 mg/mL), 10 μL of 3 M sodium acetate and 800 μL of ethanol. The precipitated DNA was washed with 100 μL of 80% cold ethanol and then dried in vacuo. The precipitated DNA was resolved in 50 μL of 10% piperidine (v/v), heated at 90 °C for 20 min and concentrated. The radioactivity of the samples was assayed using an Aloka 1000 liquid scintillation counter and the dried DNA pellets were resuspended in 80% formamide loading buffer [a solution of 80% formamide (v/v), 1 mM EDTA, 0.1% xylene cyanol and 0.1% bromophenol blue]. All reactions, along with Maxam-Gilbert G + A sequencing reactions, were heat-denatured at 90 °C for 3 min and quickly chilled on ice. The samples (1–2 μL, $2–5\times10^3$ cpm) were loaded onto 15% of polyacrylamide/7 M urea sequencing gels and electrophoresed at 1900 V for 60 min and transferred to a cassette and stored at −80 °C with Fuji X-ray film (RX-U). The gels were analyzed by autoradiography with a densitometer and BIORAD Molecular Analyst software (version 2.1). The intensity of the spots resulting from piperidine treatment was determined by volume integration.

Cleavage of ^{32}P-5′-end-labeled oligonucleotides by photoirradiation in the presence of cyanobenzophenone tethered oligodeoxynucleotides

Sample solutions were prepared by hybridizing a mixture of cold and radiolabeled oligonucleotides (**DNA 1**, 1 μM) with 1 μM of **DNA 2a** and 1 μM of **DNA 3**, **PNA 3a** or **PNA 3b**) in sodium phosphate buffer (pH 7.0). Hybridization was achieved by heating the sample at 90 °C for 5 min and slowly cooling to room temperature. The ^{32}P-5′-end-labeled ODN duplex (2.0×10^5 cpm) was irradiated at 312 nm at 0 °C for 60 min. The operation after irradiation was the same manner as described for the DNA cleavage experiment using riboflavin.

Triplex samples were prepared by hybridizing a mixture of cold and radiolabeled oligonucleotides (**DNA 4a**, 1 μM) with 1 μM of **DNA 2b** and 1 μM of **DNA 5a** and **5b** or 2 μM of **PNA 5** in sodium phosphate buffer (pH 6.2).

HOMO calculations

All calculations were performed at the B3LYP/–1G(d) level using GAUSSIAN94. Geometries of stacked base pairs were constructed as follows.[31,32] The corresponding DNA duplex dimers were built up using the Insight II program (Version 97.0) with standard B-form helical parameters which have been optimized by X-ray crystallographic analysis of relevant monomers and X-ray diffraction data of polymers.[33,34] The corresponding PNA/DNA duplex dimers were built up using the

Insight II program with helical parameters which have been optimized by NMR analysis data of polymers.[27] All the sugar backbones and peptide backbones of the duplex were replaced by methyl group at the N_1 (pyrimidine base) and N_9 (purine base). HOMO of the calculated dimers was displayed graphically using Gaussian I/F.

References and Notes

1. Hall, D. B.; Holmlin, R. E.; Barton, J. K. *Nature* **1996**, *382*, 731.
2. Burrows, C. J.; Muller, J. G. *Chem. Rev.* **1998**, *98*, 1109.
3. Grinstaff, M. W. *Angew. Chem. Int. Ed.* **1999**, *38*, 3629.
4. Núñez, M. E.; Barton, J. K. *Curr. Opin. Chem. Biol.* **2000**, *4*, 199.
5. Schuster, G. B. *Acc. Chem. Res.* **2000**, *33*, 253.
6. Giese, B. *Acc. Chem. Res.* **2000**, *33*, 631.
7. Halliwell, B.; Gutteridge, J. M. C. *Free Radicals* in *Biology and Medicine*; Oxford University Press: Oxford, 1999.
8. Melvin, T.; Plumb, M. A.; Botchway, S. W.; O'Neill, P.; Parker, A. W. *Photochem. Photobiol.* **1995**, *61*, 584.
9. Boon, P. J.; Cullis, P. M.; Symons, M. C. R.; Wren, B. W. *J. Chem. Soc., Perkin Trans. 2*, 1393.
10. Wolf, P. G.; Jones, D. D.; Candeias, L. P.; O'Neill, P. *Int. J. Rad. Biol.* **1993**, *64*, 7.
11. Steenken, S.; Jovanovic, S. V. *J. Am. Chem. Soc.* **1997**, *119*, 617.
12. Sugiyama, H.; Saito, I. *J. Am. Chem. Soc.* **1996**, *118*, 7063.
13. Saito, I.; Nakamura, T.; Nakatani, K.; Yoshioka, Y.; Yamaguchi, K.; Sugiyama, H. *J. Am. Chem. Soc.* **1998**, *120*, 12686.
14. Meggers, E.; Michel-Beyerle, M. E.; Giese, B. *J. Am. Chem. Soc.* **1998**, *120*, 12950.
15. Lewis, F. D.; Liu, X.; Liu, J.; Miller, S. E.; Hayes, R. T.; Waslelewski, M. R. *Science* **2000**, *406*, 51.
16. Nakatani, K.; Dohno, C.; Saito, I. *J. Am. Chem. Soc.* **2000**, *122*, 5893.
17. Grozema, F. C.; Berlin, Y. A.; Siebbeles, L. D. A. *J. Am. Chem. Soc.* **2000**, *122*, 10903.
18. Núñez, M. E.; Noyes, K. T.; Gianolio, D. A.; McLaughlin, L. W.; Barton, J. K. *Biochemistry* **2000**, *39*, 6190.
19. Kan, Y.; Schuster, G. B. *J. Am. Chem. Soc.* **1999**, *121*, 11607.
20. Nielsen, P. E.; Egholm, M.; Buchardt, O. *Science* **1991**, *254*, 1497.
21. Egholm, M.; Buchardt, O.; Christensen, L.; Behrens, C.; Freier, S. M.; Driver, D. A.; Berg, R. H.; Kim, S. K.; Nordén, B.; Nielsen, P. E. *Nature* **1993**, *365*, 566.
22. Armitage, B.; Ly, D.; Koch, T.; Frydenlund, H.; Ørum, H.; Batz, H. G.; Schuster, G. B. *Proc. Natl. Acad. Sci. U.S.A.* **1997**, *94*, 12320.
23. Armitage, B.; Koch, T.; Frydenlund, H.; Ørum, H.; Batz, H. G.; Schuster, G. B. *Nucleic Acids Res.* **1997**, *25*, 4674.
24. Nakatani, K.; Dohno, C.; Saito, I. *J. Org. Chem.* **1999**, *64*, 6901.
25. Koch, T.; Hansen, H. F.; Andersen, P.; Larsen, T.; Batz, H. G.; Ottesen, K.; Ørum, H. *J. Peptide Res.* **1997**, *49*, 80.
26. The circular dichromism (CD) spectra were measured at 2 °C. In CD of antiparallel DNA/PNA duplex, a strong positive band at 261 nm and a weak negative band at 240 nm were observed. The CD spectrum was in good agreement with that of DNA/PNA duplex reported earlier (Armitage, B.; Ly, D.; Koch, T.; Frydenlund, H.; Ørum, H.; Schuster, G. B. *Biochemistry* **1998**, *37*, 9417). DNA triplex exhibited a CD spectrum with a positive band at 278 nm and a negative band at 246 nm, and DNA/$(PNA)_2$ triplex exhibited a positive CD band at 275 nm and a negative CD band at 247 nm, which was consistent with that reported previously (Wittung, P.; Nielsen, P. E.; Nordén, B. *Biochemistry* **1997**, *36*, 7973).
27. Eriksson, M.; Nielsen, P. E. *Nat. Struct. Biol.* **1996**, *3*, 410.
28. Selsing, E.; Wells, R. D.; Alden, C. J.; Arnott, S. *J. Biol. Chem.* **1979**, *254*, 5417.
29. Maxam, M.; Gilbert, W. *Proc. Natl. Acad. Sci. U.S.A.* **1977**, *74*, 560.
30. Maniatis, T.; Fritsch, E. F.; Sambrook, J. *Molecular Cloning*; Cold Spring Harbor Laboratory: Plainview, New York**, 1982.**
31. Sambrook, J.; Fritsch, E. F.; Maniatis, T. *Molecular Cloning*: A Laboratory Manual, 2nd Ed., Cold Spring Harbor Laboratory: New York, 1989.
32. Yoshioka, Y.; Kitagawa, Y.; Takano, Y.; Yamaguchi, K.; Nakamura, T.; Saito, I. *J. Am. Chem. Soc.* **1999**, *121*, 8712.
33. Arnott, S.; Hukins, D. W. L. *Biochem. Biophys. Res. Commun.* **1972**, *47*, 1504.
34. Arnott, S.; Selsing, E. *J. Mol. Biol.* **1974**, *88*, 509.